PERGAMON

International Journal of Heat and Mass Transfer 45 (2002) 2213–2220

International Journal of HEAT and MASS TRANSFER

www.elsevier.com/locate/ijhmt

The onset of Darcy–Brinkman convection in a porous layer: an asymptotic analysis

D.A.S. Rees *

Department of Mechanical Engineering, University of Bath, Claverton Down, Bath BA2 7AY, UK

Received 17 March 2000; received in revised form 29 October 2001

Abstract

In highly porous media boundary (Brinkman) effects are important near impermeable surfaces. We investigate in detail how these effects modify the well-known criterion for the onset of convection of a Boussinesq fluid in a porous medium where Darcy's law applies. It is known that boundary effects serve to raise the critical Darcy–Rayleigh number as D, the Darcy number, increases. For many porous media the value of D is small and this causes severe numerical difficulties in solving the perturbation equations. We extend an earlier numerical study by Walker and Homsy [A.S.M.E. J. Heat Transfer 99 (1977) 338] by performing an asymptotic analysis of the singular perturbation problem which arises in the small-D limit. Excellent agreement is obtained between the asymptotic and numerical results. © 2002 Published by Elsevier Science Ltd.

1. Introduction

The porous medium version of the Bénard problem has been studied intensively from the mid-1940s. Since the pioneering work of Horton and Rogers [2] and Lapwood [3] the research literature has accumulated steadily. Much of the earlier work, which is described in [4,5], concentrates on cases where the Darcy-flow model is assumed to be adequate. In the last 10 years, however, there has been a great upsurge of interest in determining the effects of extensions to Darcy's law since practical applications involve media for which Darcy's law is inadequate. One of the first papers to deal with these extensions was by Vafai and Tien [6] who used macroscopic averaging techniques to determine the effects of form-drag and solid boundaries on the form of Darcy's law. Much more recently Calmidi and Mahajan [7] studied forced convection in a metal foam whose porosity is typically in the range 0.89–0.97 using the same model as [6] but supplemented by advective inertia terms. Durlofsky and Brady [8] argued that 0.95 is the lowest porosity for which the Brinkman model may be applied, but the reader is referred to the detailed discussion by Nield and Bejan [4].

In this paper, we re-examine how boundary (or Brinkman) effects affect the onset criterion in a porous layer of infinite extent. Although we also include inertia effects (both advective inertia and form-drag) in the general formulation, their presence does not affect the stability criterion since the basic state is motionless. Walker and Homsy [1] have already presented a neutral curve showing how the critical Rayleigh number varies with the Darcy number, D. This Rayleigh number is that one which is suitable for a clear-fluid, rather than for a porous medium, and therefore it increases as D decreases towards zero, the Darcy-flow limit. Here we revisit this problem, and although we present a very accurate set of numerical results, the main thrust is to provide a detailed analysis of the Darcy-flow limit. When D tends towards zero, the linearised stability equations form a singular perturbation problem and thin layers of an $O(D^{1/2})$ length-scale form near the solid boundaries. We determine the leading order correction to the Darcy-flow critical wavenumber and give the first three terms in an expansion for the critical Rayleigh number. The match between the asymptotic and the numerical results is excellent.

* Tel.: +44-(0)1225-826-775; fax: +44-(0)1225-826-928.
E-mail address: d.a.s.rees@bath.ac.uk (D.A.S. Rees).

0017-9310/02/$ - see front matter © 2002 Published by Elsevier Science Ltd.
PII: S0017-9310(01)00332-5

Nomenclature

c	specific heat
d	depth of the convection layer
D	Darcy number
f, g	linear stability variables
F, G	k-derivatives of f and g
F_1, F_2	dimensionless coefficients
$\tilde{g}$	gravity
k	wavenumber
k_m	conductivity of the porous medium
K	permeability
p	pressure
R	Darcy–Rayleigh number
t	time
T	dimensional temperature
x, y	Cartesian coordinates
u, v	fluid flux velocities

Greek symbols

α	diffusivity ratio
β	coefficient of cubical expansion
ρ	density
μ	coefficient of viscosity
μ_e	Brinkman effective viscosity
κ	diffusivity, $k_m/(\rho c)_m$
ϵ	square root of D
ψ	streamfunction
θ	scaled temperature
ϕ	porosity
ζ	scaled y coordinate

Superscripts and subscripts

$*$	dimensional
$\hat{}$	unit vector
$\bar{}$	vector
$'$	y-derivative
c	cold surface
f	fluid
h	hot surface
m	medium
$0, 1, 2$	terms in small-ϵ expansion

2. Equations of motion

It is assumed that the fluid saturating the porous medium is Boussinesq and that form-drag and boundary effects are significant. Under these circumstances the governing equations for flow and heat transfer in a porous layer are:

$$\nabla^* \cdot \underline{u}^* = 0, \tag{1a}$$

$$\frac{\rho_f}{\phi}\frac{\partial \underline{u}^*}{\partial t^*} + \frac{\rho_f}{\phi^2}(\underline{u}^* \cdot \nabla^*)\underline{u}^* = -\nabla^* p^* + \mu_e \nabla^{*2}\underline{u}^* - \left(\frac{\mu_f}{K}\right)\underline{u}^* + \rho_f \tilde{g}\beta(T - T_c)\hat{\underline{y}} - \left(\frac{\rho_f^b}{\sqrt{K}}\right)\underline{u}^*|\underline{u}^*|, \tag{1b}$$

$$(\rho c)_m \frac{\partial T}{\partial t^*} + (\rho c)_f \underline{u}^* \cdot \nabla^* T = k_m \nabla^{*2} T, \tag{1c}$$

where all constants and variables are defined in the nomenclature. Eqs. (1a)–(1c) form the full set of equations used to model convective flows in porous media. Eq. (1b) contains the usual balance of forces between viscosity and pressure gradient known as Darcy's law (viz. the 3rd and 5th terms), which is extended by the further inclusion of terms modelling in turn advective inertia (1st and 2nd terms), boundary effects (the 4th term: the Brinkman term), buoyancy (the 6th term) and form-drag (Forchheimer inertia, the 7th term). Apart from a slightly different definition of the form-drag coefficient, Eq. (1b) is the same as that given in [9] and [10], and conforms to that given by Nield and Bejan [4]. Although much work has been devoted very recently to investigating how local thermal nonequilibrium between the solid matrix and the fluid at the microscopic level affects many classical flows, we neglect this aspect here, although we note that Banu and Rees [11] consider the effect of nonequilibrium on the onset of Darcy–Bénard convection.

We consider a layer of depth, d, which is heated from below and cooled from above and no flow occurs at the boundaries. Therefore the boundary conditions are:

$$\underline{u}^* = 0, \quad T = T_h \quad \text{at } y^* = 0 \quad \text{and} \quad \underline{u}^* = 0, \quad T = T_c \quad \text{at } y^* = d. \tag{1d}$$

We have assumed that the flow is two-dimensional; in an infinite layer of constant thickness all disturbances may be Fourier-decomposed into an appropriate sum of two-dimensional modes. Nondimensionalisation proceeds using the substitutions

$$\underline{x}^* = d\,x, \quad \underline{u}^* = \frac{\kappa}{d}u, \quad t^* = \frac{\sigma d^2}{\kappa}t,$$
$$T = T_c + (T_h - T_c)\theta, \quad p^* = \rho_f \frac{\kappa^2}{d^2}p \tag{2}$$

and Eqs. (1a)–(1c) take the forms

$$\nabla \cdot \underline{u} = 0, \tag{3a}$$

$$\phi F_1 \frac{\partial \underline{u}}{\partial t} + F_1 \underline{u} \cdot \nabla \underline{u} = -\phi^2 F_1 \nabla p + D\nabla^2 \underline{u} - \underline{u} + R\theta\hat{\underline{y}} - F_2 \underline{u}|\underline{u}|, \tag{3b}$$

$$\theta_t + \underline{u} \cdot \nabla\theta = \nabla^2\theta \tag{3c}$$

subject to

$$\underline{u} = 0, \quad \theta = 1 \quad \text{at } y = 0$$
$$\text{and} \quad \underline{u} = 0, \quad \theta = 0 \quad \text{at } y = 1, \tag{3d}$$

where

$$F_1 = \frac{\rho_f \kappa K}{\phi^2 d^2 \mu_f}, \quad F_2 = \frac{\rho_f b \kappa \sqrt{K}}{d \mu_f},$$
$$R = \frac{\rho_f \tilde{g} \beta (T_h - T_c) K d}{\mu_f \kappa} \quad \text{and} \quad D = \frac{\mu_e}{\mu_f} \frac{K}{d^2}. \tag{3e}$$

In (3a)–(3e) the nondimensional coefficients F_1 and F_2 correspond to the advective and form-drag inertia terms, respectively, D is the Darcy number which usually takes very small values compared with unity, and R is the Darcy–Rayleigh number which expresses the balance between buoyancy and viscous forces. The straightforward no-flow conduction solution whose stability we analyse is given by

$$\underline{u} = 0, \quad \theta = 1 - y \tag{4}$$

and therefore we linearise Eqs. (3a)–(3e) about this solution:

$$\nabla \cdot \underline{u} = 0, \tag{5a}$$

$$\phi F_1 \frac{\partial \underline{u}}{\partial t} = -\phi^2 F_1 \nabla p + D \nabla^2 \underline{u} - \underline{u} + R \theta \underline{\hat{y}}, \tag{5b}$$

$$\theta_t - v = \nabla^2 \theta. \tag{5c}$$

We note that neither nonlinear term appears in the momentum equation, Eq. (5b), and therefore the onset criteria are independent of the size of the coefficients of these terms.

Given that the flow is two-dimensional, we introduce the streamfunction, ψ, in the usual way by defining

$$u = -\frac{\partial \psi}{\partial y}, \quad v = \frac{\partial \psi}{\partial x}, \tag{6}$$

and therefore Eqs. (5b) and (5c) reduce to

$$\phi F_1 \nabla^2 \frac{\partial \psi}{\partial t} + \nabla^2 \psi - D \nabla^4 \psi = R \frac{\partial \theta}{\partial x}, \tag{7a}$$

$$\frac{\partial \theta}{\partial t} = \nabla^2 \theta + \frac{\partial \psi}{\partial x}. \tag{7b}$$

It is straightforward to show that this system of linear equations obeys the principle of exchange of stabilities (see [12]) so that we may set the time derivatives to zero in performing the stability analysis. Therefore the system of equations we study in this paper is

$$-D \nabla^4 \psi + \nabla^2 \psi = R \frac{\partial \theta}{\partial x}, \tag{8a}$$

$$\nabla^2 \theta + \frac{\partial \psi}{\partial x} = 0 \tag{8b}$$

subject to

$$\psi = \frac{\partial \psi}{\partial y} = \theta = 0 \quad \text{at both } y = 0 \text{ and } y = 1. \tag{8c}$$

Finally we may Fourier-decompose any disturbance into an infinite set of modes in the x-direction each of which is characterised by its wavenumber, k. We substitute

$$\psi = f(y) \sin(kx), \qquad \theta = g(y) \cos(kx) \tag{9}$$

into Eqs. (8a)–(8c) to obtain

$$-D[f'''' - 2k^2 f'' + k^4 f] + [f'' - k^2 f] = -Rkg, \tag{10a}$$

$$g'' - k^2 g + kf = 0 \tag{10b}$$

subject to

$$f = f' = g = 0 \quad \text{on } y = 0 \quad \text{and} \quad y = 1. \tag{10c}$$

3. Numerical solutions

Eqs. (10a)–(10d) form an ordinary differential eigenvalue problem for R as a function of D and the wavenumber, k. When $D = 0$ we recover the Darcy-flow case which may be solved easily analytically. The addition of boundary effects renders it impossible to use entirely analytical methods and therefore we resort at first to numerical methods. As our main aim in this paper is to investigate in detail the small-D case great care must be taken in the choice of numerical method. Small values of D cause the full system to become stiff and therefore indirect methods such as the shooting method must be abandoned due to the presence of very rapidly growing components of the eigensolution. In view of this we chose to use a direct method of the same form as that used by Lewis et al. [13] and Shu and Wilkes [14].

Eqs. (10a)–(10d) were reduced to a set of three second-order equations and discretised using central differences on a uniform grid in the y-direction. The zero normal and tangential flow and zero temperature conditions provide a sufficient number of boundary conditions for these equations. However the eigenvalue, R, also needs to be found, and this requires one further condition, the normalisation condition

$$g'(0) = 1. \tag{10d}$$

When suitably arranged, the resulting set of discretised equations forms a nonlinear algebraic system. We now adopt a multidimensional Newton–Raphson iteration technique very similar indeed to that used by the Keller-box method [15] and the resulting iteration matrix has the following modified block tridiagonal form:

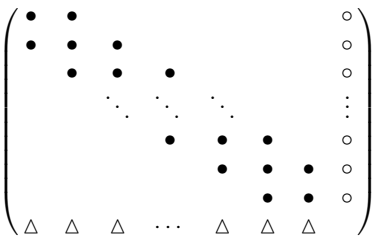

(11)

where • corresponds to 3×3 submatrix blocks arising from the differential equations, ○ to the submatrices corresponding to R-derivatives of the governing equations, and △ to the normalisation condition. Bearing in mind that the usual Keller-box methodology is used to solve parabolic systems of partial differential equations, and that this may be altered very easily to solve systems of ordinary equations with the 'streamwise' variable being replaced by a parameter which will be varied during the course of the computations, a Keller-box code was altered to be able to solve the given eigenvalue problem. As has been usual in the recent past, the author resorted to a straightforward numerical differentiation procedure to evaluate the components of the iteration matrix. Furthermore the block tridiagonal matrix algorithm had to be extended to solve the above banded matrix.

Numerical experiments indicate that the neutral stability curves always have the same qualitative form: one minimum value of R at a critical value of k with monotonic growth towards infinity as $k \to 0$ and as $k \to \infty$. Therefore it is of interest to evaluate these critical values since such a minimum value of R signifies the point above which we may expect convection to take place in an infinite layer. This is achieved by insisting that $\partial R/\partial k = 0$ and by supplementing Eqs. (10a)–(10d) by their derivatives with respect to k. Specifically, if we define

$$F = \frac{\partial f}{\partial k} \quad \text{and} \quad G = \frac{\partial g}{\partial k}, \tag{12}$$

then the differentiation of Eqs. (10a)–(10d) with respect to k yields the following system:

$$-D[F'''' - 2k^2F'' + k^4F] + [F'' - k^2F] + RkG = D[-4kf'' + 4k^3f] + 2kf - Rg, \tag{13a}$$

$$G'' - k^2G + kF = 2kg - f \tag{13b}$$

subject to the same zero boundary conditions on F, F' and G. As the wavenumber is now a second eigenvalue we also impose a second normalisation condition that $G'(0) = 0$, although any other value of this derivative would yield the same values of R and k. This new system also has an iteration matrix of the form (11) where the submatrix blocks are now 6×6.

There is now only one parameter to vary and solutions are presented for $10^{-6} \leqslant D \leqslant 10^2$. Very great care was necessary to ensure that the solutions obtained are as accurate as possible, especially for the smaller values of D where very rapid variations occur close to the bounding surfaces. To this end we used four different numerical solutions based on 200, 400, 800 and 1600 in equally spaced intervals in the range $0 \leqslant y \leqslant 1$. Given that the numerical errors in our numerical method proceed in a power series in h^2, where h is the steplength, we used Richardson extrapolation to improve the $O(h^2)$ accuracy to $O(h^4)$ in the extrapolates. These extrapolates were also subjected to the same extrapolation procedure and so on until we obtained solutions of $O(h^8)$ accuracy from the final extrapolates. In our numerical results all solutions quoted are correct to the number of places given whenever $D \geqslant 10^{-5}$; very small errors remain when $D = 10^{-6}$.

We present the variation with D of the critical values of R and k in Figs. 1 and 2. The approach to the Darcy limit as $D \to 0$ is easily seen as we recover the values, $R = 4\pi^2$ and $k = \pi$. The manner in which the approach is made is the subject of the next section as it forms a singular perturbation problem. The approach to the Bénard limit is most easily seen if we consider how R/D, the clear-fluid Rayleigh number, varies as $D \to \infty$; this is also shown in Fig. 1 and in Walker and Homsy [1] and the respective figures appear to agree very well. Here we see that the well-known rigid–rigid stability criterion given in Koschmeider [16] is obtained when ϵ is sufficiently large. Fig. 2 shows that the critical wavenumber

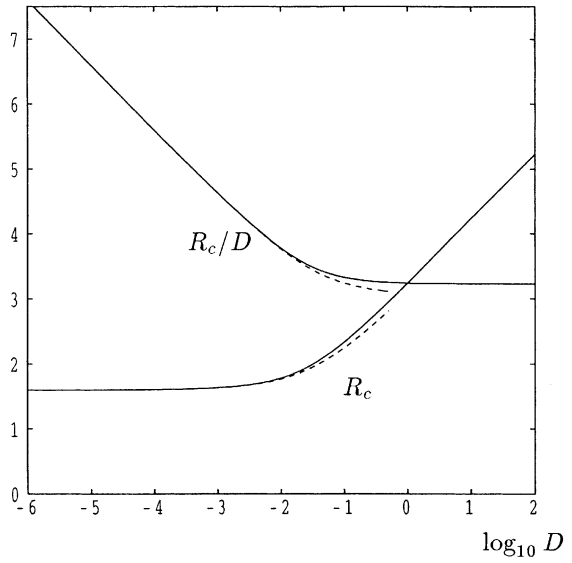

Fig. 1. Neutral curves for the onset of convection for $10^{-6} \leqslant D \leqslant 10^2$. Values are presented in terms of the Darcy–Rayleigh number, R_c, and the clear-fluid Rayleigh number R_c/D. The dashed line denotes the small-D asymptotic values given in (33).

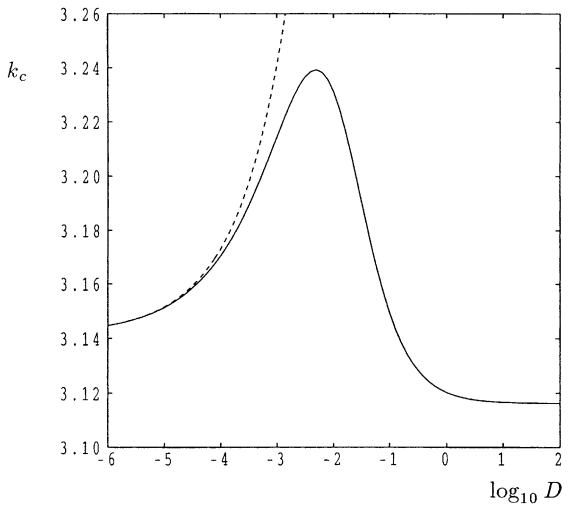

Fig. 2. Critical wavenumber, k_c, for the onset of convection for $10^{-6} \leqslant D \leqslant 10^2$. The dashed curve denotes the small-D asymptotic values given in (34).

attains a maximum value at an intermediate value of D, rather than in the limit as $D \to 0$; the physical reason for this is unknown.

Finally, we note that it is also possible to solve for R and k by applying to Eqs. (10a)–(10d) a solvability condition of the type used in the next section. That this case was realised only after the computations described above had been performed. Such a procedure again would have an iteration matrix of the form (10a)–(10d) but the submatrix blocks would only be 3×3 and the execution of the code would have been much faster.

4. Asymptotic analysis for small values of D

We now perform a singular perturbation analysis of the solution of Eqs. (10a)–(10d) as $D \to 0$. This is undertaken for general values of the wavenumber, k, and carried out as far as the third nonzero term in the expansion for R. Subsequently R is minimised with respect to k to find how R and k vary from their respective Darcy-flow values of $4\pi^2$ and π. Given that most porous media have a very small Darcy number, this analysis assumes great importance.

A detailed examination of the numerical solutions of the last section shows that very rapid variations take place close to both upper and lower surfaces which is quite standard behaviour for a singular perturbation problem. Therefore we require three asymptotic regions: the interior or main region and two thin layers near the boundaries. But given the symmetry of the layer, we need only consider the main region and the lower near-wall layer; these will be called the outer and inner regions, respectively, in accordance with standard practice. We proceed using the small parameter ϵ where

$$\epsilon^2 = D. \tag{14}$$

We will expand the solutions as power series in ϵ in the outer region:

$$\begin{pmatrix} f \\ g \end{pmatrix} = \begin{pmatrix} f_0 \\ g_0 \end{pmatrix} + \epsilon \begin{pmatrix} f_1 \\ g_1 \end{pmatrix} + \epsilon^2 \begin{pmatrix} f_2 \\ g_2 \end{pmatrix} + \cdots. \tag{15}$$

In the inner region we rescale the y-variable using the transformation

$$y = \epsilon\zeta. \tag{16}$$

This scaling for y was obtained by balancing the magnitudes of $\epsilon^2 f''''$ and f'' in Eq. (10a). In the inner region we set $f = F(\zeta)$ and $g = G(\zeta)$ and expand according to

$$\begin{pmatrix} F \\ G \end{pmatrix} = \begin{pmatrix} F_0 \\ G_0 \end{pmatrix} + \epsilon \begin{pmatrix} F_1 \\ G_1 \end{pmatrix} + \epsilon^2 \begin{pmatrix} F_2 \\ G_2 \end{pmatrix} + \cdots. \tag{17}$$

Finally we expand R using

$$R = R_0 + \epsilon R_1 + \epsilon^2 R_2. \tag{18}$$

At leading order in the outer region the equations are:

$$f_0'' - k^2 f_0 + R_0 k g_0 = 0, \tag{19a}$$

$$g_0'' - k^2 g_0 + k f_0 = 0 \tag{19b}$$

for which we take as the eigensolution

$$f_0 = \left(\frac{\pi^2 + k^2}{k}\right) \sin \pi y, \quad g_0 = \sin \pi y,$$

$$R_0 = \frac{(\pi^2 + k^2)^2}{k^2}. \tag{20}$$

This solution corresponds precisely to the usual Darcy-flow solution, but it does not satisfy the full set of boundary conditions given in (10c). The inner region is required to allow satisfaction of the $f' = 0$ conditions. From (20) we see that

$$f_0 \sim \left(\frac{\pi^2 + k^2}{k}\right) \pi y \quad \text{and} \quad g_0 \sim \pi y \tag{21}$$

as $y \to 0$, and hence the matching conditions for the inner region are

$$F \sim \left(\frac{\pi^2 + k^2}{k}\right) \pi\zeta\epsilon \quad \text{and} \quad G \sim \pi\zeta\epsilon \tag{22}$$

as $\zeta \to \infty$. Therefore the $O(\epsilon)$ terms form the leading order solutions in the inner region, and we need to take $F_0 = G_0 = 0$. The equations for F_1 and G_1 are that

$$F_1'''' + F_1'' = 0, \quad G_1'' = 0, \tag{23}$$

which must be solved subject to the matching conditions (22) and the boundary conditions $F_1(0) = F_1'(0) = G_1(0) = 0$. We find that

$$F_1 = \pi\left(\frac{\pi^2+k^2}{k}\right)(\zeta + \mathrm{e}^{-\zeta} - 1), \quad G_1 = \pi\zeta, \tag{24}$$

which shows that the inner region is passive with respect to G to this order.

The $O(\epsilon)$ solution for F_1 forces a solution of the same magnitude in the outer region. The equations for f_1 and g_1 are:

$$f_1'' - k^2 f_1 + R_0 k g_1 = -R_1 k g_0, \tag{25a}$$

$$g_1'' - k^2 g_1 + k f_1 = 0 \tag{25b}$$

subject to the matching conditions

$$f_1(0) = -\pi\left(\frac{\pi^2+k^2}{k}\right), \quad g_1(0) = 0, \tag{25c}$$

which were obtained from (24). As R_1 multiplies a term which forms part of the eigensolution of the equivalent homogeneous system, it is necessary to derive a solvability condition. If both the boundary conditions given in (25c) had been homogeneous, then solvability would correspond simply to $R_1 = 0$, which removes the resonant term. In the present case it is easy to show that

$$\int_0^1 ([f_1'' - k^2 f_1 + R_0 k g_1] f_0 + R_0[g_1'' - k^2 g_1 + k f_1] g_0)\,\mathrm{d}y = f_1(0) f_0'(0) - f_1(1) f_0'(1) \tag{26}$$

using integration by parts and noting that f_0 and g_0 satisfy (19a) and (19b). Substitution of (25a)–(25c) into (26) yields

$$-R_1 k \int_0^1 g_0 f_0\,\mathrm{d}y = -2\pi^2\left(\frac{\pi^2+k^2}{k}\right)^2 \tag{27}$$

and hence that

$$R_1 = \frac{4\pi^2(\pi^2+k^2)}{k^2}. \tag{28}$$

Given this value of R_1 we may solve Eqs. (25a)–(25c) to obtain

$$f_1 = \frac{\pi}{2k}(\pi^2+k^2)\left[2\left(y-\frac{1}{2}\right)\cos\pi y - \frac{\cosh\lambda\left(y-\frac{1}{2}\right)}{\cosh\frac{1}{2}\lambda}\right], \tag{29a}$$

$$g_1 = -\frac{2\pi^2}{\pi^2+k^2}\sin\pi y + \frac{\pi}{2}\left[2\left(y-\frac{1}{2}\right)\cos\pi y + \frac{\cosh\lambda\left(y-\frac{1}{2}\right)}{\cosh\frac{1}{2}\lambda}\right], \tag{29b}$$

where $\lambda = \sqrt{2k^2+\pi^2}$.

Omitting further details we find that the $O(\epsilon^2)$ inner solution is now

$$F_2 = \frac{\pi}{k}(\pi^2+k^2)\left[1+\frac{1}{2}\lambda\tanh\frac{1}{2}\lambda\right][\zeta + \mathrm{e}^{-\zeta} - 1], \tag{30a}$$

$$G_2 = \left[\pi\left(\frac{k^2-\pi^2}{k^2+\pi^2}\right) - \frac{1}{2}\pi\lambda\tanh\frac{1}{2}\lambda\right]\zeta. \tag{30b}$$

Finally, at $O(\epsilon^2)$ in the outer region, we obtain a very lengthy equation for f_2 and g_2 which involves R_2. On application of a solvability condition of the same type as above we obtain

$$R_2 = \frac{(\pi^2+k^2)^3}{k^2} + \frac{4\pi^2}{k^2}\left(1+\frac{1}{2}\lambda\tanh\frac{1}{2}\lambda\right) + \frac{2\pi^2}{k^2}(3\pi^2+k^2). \tag{31}$$

We now have analytical expressions for the first three terms in the asymptotic expansion for the neutral Rayleigh number for general values of k. The critical value is obtained by minimising with respect to k. If we set $k = \pi + \epsilon k_1$ into the full expression for $R = R_0 + \epsilon R_1 + \epsilon^2 R_2$ obtained using (20), (28) and (31), and expand the resulting series, then we obtain

$$R \sim 4\pi^2 + [8\pi^2]\epsilon + [8\pi^4 + 16\pi^2 + 4\pi^3\sqrt{3}\tanh(\sqrt{3}\pi/2) + 4k_1^2 - 8\pi k_1]\epsilon^2. \tag{32}$$

The coefficient of ϵ^2 is minimised when $k_1 = \pi$ and therefore we obtain the following critical values for R and k:

$$R_c \sim 4\pi^2 + [8\pi^2]\epsilon + [8\pi^4 + 12\pi^2 + 4\pi^3\sqrt{3}\tanh(\sqrt{3}\pi/2)]\epsilon^2, \tag{33}$$

$$k_c \sim \pi + \epsilon\pi. \tag{34}$$

Comparison with the numerical solution may be aided if (33) is written in the form

$$\frac{R_c}{4\pi^2} \sim 1 + 2\epsilon + \left[2\pi^2 + 3 + \pi\sqrt{3}\tanh(\sqrt{3}\pi/2)\right]\epsilon^2 = 1 + 2\epsilon + 28.1337\epsilon^2. \tag{35}$$

A graphical comparison of the critical values of R and k given in (33) and (34) with those computed numerically are shown in Figs. 1 and 2, and it is clear that the two approaches agree exceptionally well for $D < 10^{-2}$ for the Rayleigh number and for $D < 10^{-4}$ for the wavenumber. This agreement may be judged quantitatively in Tables 1 and 2 which show the thrice-extrapolated numerical solutions. Table 1 is concerned with the critical Rayleigh number. Here the numerical solutions have been processed in such a way that the coefficient of ϵ^2 in (35) should be the value of the entries in the final column of the table if (35) were exact, rather than being the first three terms in an asymptotic expansion. We see that the comparison is also excellent, although the entry for $D = 10^{-6}$ is not so good – this is

Table 1
Comparison of the exact and asymptotic values of the critical Rayleigh number as a function of $D = \epsilon^2$

D	R_c	$R_c/4\pi^2$	$(R_c/4\pi^2 - 1 - 2\epsilon)$	$(R_c/4\pi^2 - 1 - 2\epsilon)/\epsilon^2$
10^{-3}	43.149043	1.0929780	0.0297324	29.734
10^{-4}	40.381006	1.0228628	0.0028628	28.628
10^{-5}	39.739268	1.0066074	0.0002828	28.28
10^{-6}	39.558118	1.0020188	0.0000188	18.8

R_c denotes the computed value of the Rayleigh number. The final column should yield the value 28.1337 (see Eq. (35)) as $D \to 0$.

Table 2
Comparison of the exact and asymptotic values of the critical wavenumber as a function of $D = \epsilon^2$

D	k_c	k_c/π	$(k_c/\pi - 1 - \epsilon)$	$(k_c/\pi - 1 - \epsilon)/\epsilon^2$
10^{-3}	3.214410	1.023178	−0.008444	−8.444
10^{-4}	3.170412	1.009174	−0.000827	−8.27
10^{-5}	3.151272	1.003081	−0.000081	−8.1
10^{-6}	3.144694	1.000987	−0.000013	−13.0

k_c denotes the computed value of the wavenumber. The final column demonstrates that the $O(\epsilon)$ solution given in (34) has an $O(\epsilon^2)$ error.

due to the decreasingly good resolution of the near-wall layers. A similar phenomenon is found in Table 2 which depicts the analogous comparison for the critical wavenumber. The final column now corresponds to the $O(\epsilon^2)$ correction to the Darcy value. We see that the coefficient of ϵ^2 is approximately -8.

5. Conclusion

In this paper, we have analysed in detail the numerical data presented originally by Walker and Homsy [1] for the onset of convection of a Darcy–Brinkman fluid in a horizontal layer. We find that the resulting singular perturbation problem may be solved by invoking the existence of a layer of $O(D^{1/2})$ thickness near the upper and lower surfaces. We have obtained an expansion for the critical Rayleigh number which is correct to three terms and for the wavenumber to two terms. These compare very well indeed with our detailed numerical results which were obtained using a modified form of the Keller-box scheme and three improvements using Richardson's extrapolation technique.

The present work may be extended in various ways. Kladias and Prasad [9,10] have considered strongly nonlinear convection and the onset of unsteady convection, but have restricted their study to two-dimensional flows in square cavities. It will be important to consider cavities of other aspect ratios, and to allow three-dimensionality. Another important case is the determination of the stability characteristics of weakly nonlinear convection. In other contexts it is possible for roll patterns to be unstable in general with cells of square planform forming the stable convection pattern; see [17,18] for example. In the present context it is well-known that rolls form the stable pattern in both the large-D and small-D limits, but the nature of the stable pattern at intermediate values of D is not known. A third case is the determination of how boundary effects modify the stability characteristics of convection in a vertical porous layer. Kwok and Chen [19] studied this problem using fully numerical methods and determined a criterion for the onset of convection. However, an earlier paper by Gill [20] showed analytically that Darcy-flow ($D = 0$) is stable in this configuration. At present it is unknown how small D must become before stability is re-established.

Acknowledgements

The author would like to thank the referees for their very helpful comments.

References

[1] K. Walker, G.M. Homsy, A note on convective instabilities in Boussinesq fluids and porous media, A.S.M.E. J. Heat Transfer 99 (1977) 338–339.
[2] C.W. Horton, F.T. Rogers, Convection currents in a porous medium, J. Appl. Phys. 16 (1945) 367–370.
[3] E.R. Lapwood, Convection of a fluid in a porous medium, Proc. Cambridge Philos. Soc. 44 (1948) 508–521.
[4] D.A. Nield, A. Bejan, Convection in Porous Media, second ed., Springer, New York, 1999.
[5] D.A.S. Rees, The stability of Darcy–Bénard convection, in: K. Vafai, H. Hadim (Eds.), Handbook of Porous Media, vol. 12, Dekker, New York, 2000, pp. 521–528.
[6] K. Vafai, C.L. Tien, Boundary and inertia effects on flow and heat transfer in porous media, Int. J. Heat Mass Transfer 24 (1981) 195–203.

[7] V.V. Calmidi, R.J. Mahajan, Forced convection in high porosity metal foams, A.S.M.E. J. Heat Transfer 122 (2000) 557–565.
[8] L. Durlofsky, J.F. Brady, Analysis of the Brinkman equation as a model for flow in porous media, Phys. Fluids 30 (1987) 3329–3341.
[9] N. Kladias, V. Prasad, Natural convection in horizontal porous layers: effects of Darcy and Prandtl numbers, A.S.M.E. J. Heat Transfer 111 (1989) 926–935.
[10] N. Kladias, V. Prasad, Flow transitions in buoyancy-induced non-Darcy convection in a porous medium heated from below, A.S.M.E. J. Heat Transfer 112 (1990) 675–684.
[11] N. Banu, D.A.S. Rees, The onset of Darcy–Bénard convection using a thermal nonequilibrium model, Int. J. Heat Mass Transfer 45 (2002) 2221–2228.
[12] P.G. Drazin, W.H. Reid, Hydrodynamic Stability, Cambridge University Press, Cambridge, 1981.
[13] S. Lewis, D.A.S. Rees, A.P. Bassom, High wavenumber convection in tall porous containers heated from below, Q. J. Mech. Appl. Math. 50 (1997) 545–563.
[14] J.J. Hsu, G. Wilkes, Mixed convection laminar film condensation on a semi-infinite vertical plate, J. Fluid Mech. 300 (1995) 207–229.
[15] T. Cebeci, P. Bradshaw, Physical and Computational Aspects of Convective Heat Transfer, Springer, New York, 1984.
[16] E.L. Koschmeider, Bénard cells and Taylor vortices, Cambridge Monographs on Mechanics and Applied Mathematics, Cambridge, 1993.
[17] D.N. Riahi, Nonlinear convection in a porous layer with finite conducting boundaries, J. Fluid Mech. 129 (1983) 153–171.
[18] D.A.S. Rees, D.S. Riley, The three-dimensional stability of finite-amplitude convection in a layered porous medium heated from below, J. Fluid Mech. 211 (1990) 437–461.
[19] L.P. Kwok, C.F. Chen, Stability of thermal-convection in a vertical porous layer, A.S.M.E. J. Heat Transfer 109 (1987) 889–893.
[20] A. Gill, Stability of convection in a vertical porous slab, J. Fluid Mech. 35 (1969) 545–546.